Environ. Sci. Technol. **2000**, *34,* 130−136

Kinetics of MSWI Fly Ash Thermal Degradation. 1. Empirical Rate Equation for Native Carbon Gasification

MARINA LASAGNI, ELENA COLLINA, MASSIMO TETTAMANTI, AND DEMETRIO PITEA*

Dipartimento di Scienze dell'Ambiente e del Territorio (DISAT), Universitá degli Studi di Milano-Bicocca, Piazza della Scienza 1, 20126 Milano, Italy

The thermal degradation rate of organic carbon on fly ashes from different municipal solid waste incinerators, MSWIs, is studied in batch experiments in air. A global parameter, total organic carbon (TOC), is used to measure the decrease of reagent concentration in time. The TOC vs time data are well fitted by deconvolution treatment with a sum of two first-order reactions, Ri and Rj. To identify the limits of deconvolution, kinetics of the model systems dibenzofuran (DF)−biphenyl (BPh)−SiO_2 and DF−BPh−active carbon−SiO_2 are studied. Both Ri and Rj are carbon oxidation reactions to CO_2, the oxidized carbon being not from adsorbed organic compounds but from the native carbon matrix of MSWI fly ash. Large negative $\Delta S^{\ddagger}$ values indicate that Ri and Rj transition states are more compact and stiffer than the reagent ones. Structural changes are more important than chemical transformations since the entropic term is predominant in determining the $\Delta G^{\ddagger}$ values. The key experimental information for the formulation of a generalized kinetic model and a mechanism for carbon gasification (Part 2) is the temperature dependence of the preexponential parameters in the empirical rate equation.

Introduction

Since the late 1970s it is well-known that solid, liquid, and gaseous emissions from incinerators contain many different classes of organic compounds, halogenated derivatives included, among which polychlorinated dibenzo-*p*-dioxins (PCDD) and polychlorinated dibenzofurans (PCDF) have been demonstrated to be particularly dangerous for human health and the environment *(1)*.

Literature data *(2)* clearly indicate that fly ashes collected in the energy recovery and environmental control units, called "cold zones", contain significant concentrations of PCDD and PCDF even if such pollutants are totally absent or present only in traces at the outlets of the combustion and post-combustion chambers. This observation suggests that these compounds are formed after the combustion zones, involving lower temperatures and probably two mechanisms on fly ash surface: (i) formation from precursors, i.e. chloroaromatic molecules such as polychlorobenzenes and polychlorophenols and (ii) *de novo* synthesis, starting from more or less complex non-chlorinated molecules, native carbon included, and a chlorine source such as Cl_2, HCl, or inorganic chlorides. In both cases, fly ash can act as a catalyst; at least in the latter mechanism, oxygen is essential.

In nitrogen, no PCDD or PCDF forms, whereas, already with 1% oxygen, their formation is observed *(3, 4)*.

As for carbon, Ismail and Walker *(5)* have shown that at 77 °C the interaction of O_2 with Saran char is due to physical and chemical oxygen adsorption, while at 100 °C only oxygen chemisorption is detected. Between 125 °C and at least 227 °C, oxygen interaction with the char results in two concurrent reactions, oxygen chemisorption and char gasification. By comparing the char gasification rates estimated from these low temperatures data with those predicted by extrapolation of high temperature (450−550 °C) experiments, the authors suggested that super active sites exist at low temperatures which are rapidly annealed out at higher temperatures.

Stieglitz and co-workers *(6, 7)* showed that CO_2 is evolved from carbon in municipal solid waste incinerator, MSWI, fly ash at temperatures near 300 °C. Evidence for gasification of native carbon in MSWI fly ash is reported by Milligan and Altwicker *(8, 9)*; their experiments were performed under an air flow in a fixed bed reactor. They found that the gasification rates depend on the initial carbon content (about 2% and 7%) and are an order of magnitude greater for the higher concentration. Another noticeable feature is that the gasification rates of native carbon in toluene-extracted fly ashes were at least an order of magnitude greater than those of pure activated carbon; however, when activated carbon was added to fly ash, an increase of more than an order of magnitude in gasification rates was observed when compared with its pure form. Based on these different reactivities, a catalytic gasification mechanism was hypothesized as well as a possible role of carbon morphology, as similar effects were not observed with carbon black.

In a recently published paper on the mechanism of *de novo* synthesis of PCDD/PCDF *(10)*, Huang and Buekens report an excellent overview of catalyzed and uncatalyzed mechanisms of carbon gasification in the low-temperature range (200−500 °C). They suggest that in order to understand the *de novo* synthesis reaction, it is necessary to understand the carbon gasification reaction, especially the O_2 mode of attack on graphitic carbon structures.

In the past few years, thermal behavior of fly ash has been extensively studied *(11, 12)*. Most studies have focused on PCDD and PCDF formation, whereas the other somewhat more abundant and less toxic compounds have usually not been taken into account. Fly ash contains both organic compounds and unburned unextractable carbon (native carbon). We decided to focus our attention on their reactions and are doing kinetic work on the thermal behavior of MSWI raw fly ash as well as model systems with PCDD, PCDF, PCB parent compounds, i.e. Dibenzo-*p*-Dioxin, DD, Dibenzo-Furan, DF, and BiPhenyl, BPh, and activated carbon, C, mixed with silica, SiO_2. The model mixtures were studied to gain information on the thermal behavior of single compounds and on their reactivity *(13)*.

As for fly ash, it is quite difficult to study and interpret the kinetics and mechanism of thermal degradation of a single organic compound in such a complex system. To overcome this difficulty, we investigated the possibility of using a lump parameter such as total organic carbon, TOC, to follow the concentration decrease of organics and native carbon and set up a method for measuring TOC directly on a solid matrix *(14−16)*. Of course, due to the complexity and the use of a global parameter, specificity is partially lost. However, once

* Corresponding author phone: +39-02-26603253; fax: +39-02-70638129; e-mail: d.pitea@csrsrc.mi.cnr.it.

10.1021/es981264c CCC: $19.00
Published on Web 12/02/1999

TABLE 1. Products of 3 h Thermal Treatment of About 5 g of Fly Ash at Different Temperatures[a]

sample	run	air/N_2	T (°C)	TOC° ($t = 0$) (ppm)	TOC ($t =$ 3 h) (%)	CO_2 (%)	recovery (%)
FA1	1	air	250	2230	71	15	86[b]
FA1	2	air	325	2230	69	10	79[b]
FA1	3	air	500	2230	6	94	100
FA2a	4	air	250	2165	82	12	94
FA2a	5	air	500	2165	24	71	95
FA2b	6	air	250	7820	28	70	98[b]
FA2b	7	air	500	7820	25	78	103
FA3	8	air	350	3525	72	28	100[b]
FA3	9	air	500	3525	12	90	102
FA1	10	N_2	150	2230	100		100
FA1[a]	11	N_2	200	2230	99		99[b]
FA1	12	N_2	200	2230	90	6	96[b]
FA2b	13	N_2	200	7820	96		96[b]
FA2b	14	N_2	500	7820	91	4	95[b]
FA3	15	N_2	200	3525	96		96[b]
FA3	16	N_2	500	3525	89	6	95

[a] The percent values are calculated with respect to of TOC at $t = 0$ (TOC°). [b] Traces of organic compounds (see text). [c] Thirty min thermal treatment.

the global behavior is understood, detailed information can be obtained by performing specific studies.

In the present work, the results of batch experiments performed on both raw fly ash and model systems DF−BPh−SiO_2 and DF−BPh-C−SiO_2 are reported, and an empirical kinetic equation is formulated. In part 2 (*17*), a general reaction scheme based on the experimental data is proposed and used to determine fly ash native carbon gasification rates. Batch experiments can be particularly useful to understand the reactivity of combustion wall deposits. Moreover, to correlate kinetic results with fly ash properties, we are studying both native carbon properties and fly ash structure and composition *(18)*. The results already obtained and those we hope will bear fruit are in the fields of (i) basic research on reaction pathways, kinetics, and mechanisms as well as energy aspects of reactions on fly ash and (ii) technological applications on the MSW incineration process as well as thermal fly ash treatments for final disposal.

Experimental and Results

Reagents and Materials. SiO_2 (Merck, grade 60, 230-40 Mesh ASTM), DF and BPh (Janssen purity 99+% and 99%), and C (Fluka, purum) were used without any further treatment. Mixtures DF−BPh−SiO_2 (initial TOC content due to DF, $TOC^0_{DF} = 1775$ ppm and to BPh, $TOC^0_{BPh} = 1775$ ppm) and DF−BPh−C−SiO_2 ($TOC^0_{DF} = 630$, $TOC^0_{BPh} = 320$, and $TOC^0_C = 920$ ppm) were prepared as previously reported *(13)*.

Fly ash was collected from modern waste incinerator ESP hoppers in Denmark (FA1: Reno-Nord and FA2a and FA2b: Reno-Syd) and in Italy (FA3: AMSA, Milan, via Zama). Each sample was homogenized using a ball mill (Retsch, Model S1) operating with three 10 mm-∅ balls and two 20 mm-∅ ones at 80 rpm for 25 min. It was then dried and used for the experiments without further treatment: the initial TOC content, TOC^0, of each sample is reported in Table 1.

FA30, taken from the FA3 sample, was dried and used without homogenization ($TOC^0 = 3430$ ppm); FA3E was exhaustively Soxhlet extracted with toluene for 24 h, dried, and then homogenized ($TOC^0 = 2870$ ppm).

The TOC was measured using a Dohrmann instrument assembled with the Standard Module, DC-90, the Purgeable Organics Module, PRG-1, and the Sludge Sediment Sampler Accessory, S/SS. Details of the analytical method have already been reported *(14−16)*.

Reaction Products in Air and Analytical Procedures. To identify the reaction products in air, samples of about 5 g of fly ashes from different origins were treated for 3 h in the 250−500 °C temperature range in a fixed-bed reactor system (*13*) kept closed (reactor volume, 35 cm^3). After the treatment, nitrogen (100 mL/min) flowed through the reactor for 1 h, bubbling in a series of five impingers, the first filled with cyclohexane, and the following four with a saturated $Ba(OH)_2$ solution. Preliminary experiments as well as the reaction yields showed that this is an effective way to collect the organics and carbon dioxide formed under reaction conditions.

To identify organic products, the cyclohexane trap was analyzed with a HP 5890 gas chromatograph (CP-Sil 8 CB column, Chrompack) coupled to a HP 5970 mass selective detector. The temperature program was 1 min at 60 °C, then 20 °C min^{-1} to 280 °C, and 5 min at 280 °C. To determine the carbon dioxide developed in the reaction, the four $Ba(OH)_2$ solutions and a blank were titrated with HCl 0.5 N. The residual TOC content of the sample was also determined. Previous experiments *(15, 16)* showed that inorganic carbon content of fly ash is less than 5% of the total carbon present: thus, TOC is a good and quick parameter to measure the fly ash organic carbon content variations during thermal reactions.

Table 1 reports the products distribution of the fly ash reactions in air at the various temperatures (runs 1−9). In any case, CO_2 was the main product; the CO/CO_2 ratio was quantitatively determined by gas chromatographic analyses: in any experimental condition, the ratio was lower than 0.05; literature data on low-temperature carbon gasification *(10)* confirm that the gasification product is mainly CO_2.

At temperatures below 250 °C, even with a 24 h reaction time, the difference between initial and final TOC content was less than 5%, i.e., the same as the analytical method detection limit *(15, 16)*. In the temperature range 250−325 °C (Table 1, runs 1, 2, 6, and 8) traces of several organic compounds were detected in the organic solvent impinger. The compounds were identified by comparing the registered spectra with the spectra stored in the software library (NBS43K.1). The trace organics are quite distinct: FA1 mainly gives tetra- to hexachlorobenzenes, whereas FA2b gives hexadecane and heptane and FA3, tetrachloroethane, and dichlorobenzene.

At higher temperatures (runs 3, 5, 7, and 9), the TOC decrease is quantitative; the gasification product is mainly CO_2. Under these conditions, organic compounds were not detected in the flue gases.

The products of the thermal treatment of DF−BPh−SiO_2 and DF−BPh−C−SiO_2 mixtures were desorbed DF and BPh and CO_2 from the combustion of C *(13)*.

Reaction Products in Nitrogen. To study the role of organic compounds desorption on kinetics, 5 g of FA1 or FA2b or FA3 samples were treated at different temperatures in a nitrogen flow (100 mL/min). The products were analyzed as described; results are reported in Table 1 (runs 10−16).

At 150 °C (run 10), no desorption or reaction occurred, while in the other runs there were traces of unidentified organic compounds. In any case, the recovery was at least 95%. A qualitative analysis of the chromatogram patterns showed that the same organics with a constant concentration ratio were desorbed from FA1 at 200 °C and different reaction times (runs 11 and 12); thus, half an hour was sufficient for complete desorption. Results of runs 13 and 14 on FA2b or 15 and 16 on FA3 showed that the concentration ratio (measured as the chromatographic peaks ratio) of the compounds already desorbed at 200 °C did not change at 500 °C. In addition, new compounds were present at the higher temperature. The desorbed compound typology was temperature and fly ash dependent.

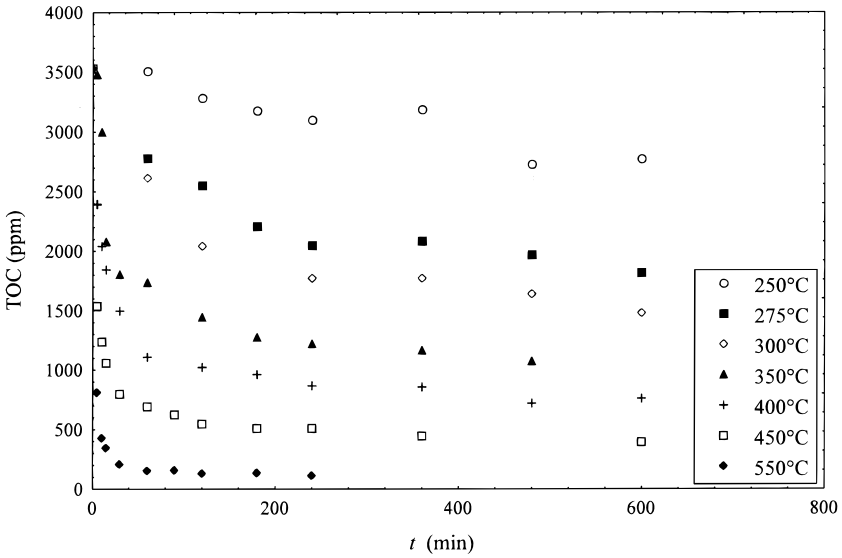

FIGURE 1. TOC-time data at selected temperatures for the thermal treatment of FA3.

TABLE 2. Deconvolution Parameters C_i, k_i, C_j, and k_j Calculated for Reactions Ri and Rj of FA1 at Different Temperatures

T (°C)	$C_i \pm \sigma$ (ppm)	$k_i \pm \sigma$ (min^{-1})	$C_j \pm \sigma$ (ppm)	$k_j \pm \sigma$ (min^{-1})	R^2 deconvolution	R^2 first-order eq
225	1939 ± 41	(1.0 ± 0.3) 10^{-4}	297 ± 39	(1.0 ± 0.3) 10^{-2}	0.990	0.776
275	1868 ± 43	(4.5 ± 0.4) 10^{-4}	378 ± 54	(1.6 ± 0.4) 10^{-2}	0.991	0.937
375	594 ± 78	(7 ± 3) 10^{-4}	1631 ± 72	(1.8 ± 0.2) 10^{-2}	0.998	0.778
400	355 ± 191	(3 ± 2) 10^{-3}	1861 ± 185	(2.3 ± 0.3) 10^{-2}	0.997	0.780
500	233 ± 71	(2 ± 1) 10^{-3}	1990 ± 74	(2.7 ± 0.2) 10^{-2}	0.998	0.713
600	280 ± 93	(3 ± 1) 10^{-3}	1944 ± 98	(3.2 ± 0.3) 10^{-2}	0.997	0.698

Kinetic Runs. The samples (about 2 g) were thermally treated in air in a closed muffle furnace, internal volume 9 L. The temperature was determined by a thermocouple located at the top of the reaction vessel; isothermal temperature control was ±5 °C at 350 °C. The oxygen (25 mmol) was present in great excess; for $TOC^0 = 8000$ ppm, the molar ratio O_2/C is about 20. Due to this excess, the oxygen concentration is practically unchanged under every experimental condition. The reaction temperature ranged from 75 to 600 °C. The reaction times varied from 5 to 1440 min. At each kinetic time, the residual TOC content of the sample was determined.

Details of TOC content variation in time at different temperatures for the overall kinetic runs (above 50) performed on fly ash and DF−BPh−SiO_2 or DF−BPh−C−SiO_2 mixtures are available as Supporting Information. To show typical trends, data for FA3 are reported in Figure 1.

Kinetic Data Processing

Fly Ash Kinetics. The experimental data for the TOC decrease in time were processed with standard kinetic schemes. In addition, the first-order kinetics observed for single compounds on SiO_2 *(13)* and the fact that TOC is a lump-parameter (i.e., every organic present in the sample contributes to the TOC value) were taken into account. So, two kinetic equations were finally considered: a standard first-order kinetics and a sum of two exponentials:

$$\mathrm{TOC} = C_i \exp(-k_i t) + C_j \exp(-k_j t) \qquad (1)$$

C_i and C_j are "preexponential factors" (at time $t = 0$, $C_i + C_j = TOC^0$); k_i and k_j are the rate constants of the two reactions, named Ri and Rj; conventionally, the higher rate constant is called k_j. The "best" values of the parameters minimizing the residual sum of squares were calculated iteratively starting from guess values. The nonlinear estimation procedure was the Simplex method with a quasi-Newton method *(19)*. In the following, this procedure is referred to as "deconvolution". Tables 2−5 report the rate constants, k_i and k_j, together with C_i and C_j values. To estimate the goodness of fit, both the parameters standard errors, σ, and the coefficient of determination (R^2) are reported; for the sake of comparison, the tables also show the R^2 obtained with the first-order kinetic scheme. Sensitivity analysis was conducted by varying the set of initial parameter estimates.

The apparent activation and thermodynamic parameters calculated using Arrhenius and Eyring equations are reported in Table 6; the goodness of fit is evaluated on the basis of the standard deviation of the least-squares regression parameters as well as the determination coefficients (R^2).

To verify whether two activation or thermodynamic parameters were significantly different, a statistical procedure for comparing slopes and intercepts of the regression lines was applied at 95% confidence level *(20)*. Two values are considered "not different" if the statistical test indicates that the null hypothesis H_0 (the two values are not different at a 95% confidence level) must be accepted; on the contrary, if H_0 is rejected, the two values are "different".

DF−BPh−SiO_2 and DF−BPh−C−SiO_2 Mixtures Kinetics. The experimental data for the DF−BPh−SiO_2 and DF−BPh−C−SiO_2 mixtures reactions were fitted both by the first-order kinetic scheme and the deconvolution procedure. The calculated deconvolution parameters C_i and C_j and the rate constants, k_i and k_j (min^{-1}), together with the first-order rate constants, k^{mix2} (min^{-1}) for DF−BPh−SiO_2 mixture and k^{mix3} (min^{-1}) for DF−BPh−C−SiO_2 mixture, are reported in Table 7. The parameters standard errors, σ, and the R^2 are also reported. Table 8 gives the activation and thermodynamic

TABLE 3. Deconvolution Parameters C_i, k_i, C_j, and k_j Calculated for Reactions Ri and Rj of FA2a at Different Temperatures

T (°C)	$C_i \pm \sigma$ (ppm)	$k_i \pm \sigma$ (min^{-1})	$C_j \pm \sigma$ (ppm)	$k_j \pm \sigma$ (min^{-1})	R^2 deconvolution	R^2 first-order eq
200	2097 ± 37	(7 ± 2) 10^{-5}	84 ± 44	(7 ± 6) 10^{-3}	0.947	
250	1831 ± 32	(1.2 ± 0.2) 10^{-5}	340 ± 42	(1.1 ± 0.3) 10^{-2}	0.988	
275	1648 ± 62	(3.2 ± 0.5) 10^{-5}	522 ± 70	(1.0 ± 0.3) 10^{-2}	0.991	0.864
325	871 ± 98	(3 ± 2) 10^{-4}	1257 ± 104	(1.5 ± 0.3) 10^{-2}	0.989	0.615
350	896 ± 73	(4 ± 2) 10^{-4}	1247 ± 95	(2.6 ± 0.6) 10^{-2}	0.983	0.538
400	764 ± 86	(7 ± 3) 10^{-4}	1370 ± 122	(5 ± 1) 10^{-2}	0.973	0.493
450	569 ± 86	(4 ± 3) 10^{-4}	1531 ± 128	(8 ± 2) 10^{-2}	0.973	0.386
475	530 ± 30	(3 ± 1) 10^{-4}	1615 ± 62	(1.6 ± 0.2) 10^{-1}	0.991	0.300
550	428 ± 38	(2 ± 1) 10^{-3}	1737 ± 53	(3.1 ± 0.3) 10^{-1}	0.998	0.452
600	555 ± 50	(1.1 ± 0.3) 10^{-2}	1610 ± 62	(9 ± 6) 10^{-1}	0.999	0.576

TABLE 4. Deconvolution Parameters C_i, k_i, C_j, and k_j Calculated for Reactions Ri and Rj of FA2b at Different Temperatures

T (°C)	$C_i \pm \sigma$ (ppm)	$k_i \pm \sigma$ (min^{-1})	$C_j \pm \sigma$ (ppm)	$k_j \pm \sigma$ (min^{-1})	R^2 deconvolution	R^2 first-order eq
350	5575 ± 106	(1.0 ± 0.2) 10^{-4}	2186 ± 115	(1.3 ± 0.2) 10^{-2}	0.994	0.565
400	4575 ± 103	(1.0 ± 0.2) 10^{-4}	3227 ± 111	(1.09 ± 0.09) 10^{-2}	0.998	0.523
450	3149 ± 169	(3.4 ± 0.9) 10^{-4}	4703 ± 218	(1.8 ± 0.2) 10^{-2}	0.995	0.563
500	2485 ± 738	(1.3 ± 0.8) 10^{-3}	5502 ± 820	(2.1 ± 0.6) 10^{-2}	0.979	0.851
600	2507 ± 1053	(4 ± 2) 10^{-3}	5386 ± 1102	(3.0 ± 0.8) 10^{-2}	0.949	0.949

TABLE 5. Deconvolution Parameters C_i, k_i, C_j, and k_j Calculated for Reactions Ri and Rj of FA3, FA30, and FA3E at Different Temperatures

T (°C)	$C_i \pm \sigma$ (ppm)	$k_i \pm \sigma$ (min^{-1})	$C_j \pm \sigma$ (ppm)	$k_j \pm \sigma$ (min^{-1})	R^2 deconvolution	R^2 first-order eq
			FA3			
275	2014 ± 109	(10 ± 6) 10^{-5}	1498 ± 123	(10 ± 2) 10^{-3}	0.986	0.524
300	1716 ± 100	(1.2 ± 0.7) 10^{-4}	1816 ± 127	(1.2 ± 0.2) 10^{-2}	0.991	0.497
350	1388 ± 152	(3 ± 2) 10^{-4}	2312 ± 236	(5 ± 1) 10^{-2}	0.955	0.424
400	1062 ± 100	(4 ± 2) 10^{-4}	2327 ± 158	(8 ± 2) 10^{-2}	0.977	0.423
450	704 ± 88	(8 ± 4) 10^{-4}	2776 ± 161	(2.0 ± 0.3) 10^{-1}	0.979	0.314
550	304 ± 50	(6 ± 2) 10^{-3}	3219 ± 70	(3.6 ± 0.3) 10^{-1}	0.998	0.476
			FA30			
300	1970 ± 266	(2 ± 1) 10^{-4}	1478 ± 325	(1.0 ± 0.5) 10^{-2}	0.931	
400	1330 ± 124	(5 ± 2) 10^{-4}	2020 ± 188	(9 ± 2) 10^{-2}	0.966	
500	844 ± 194	(3 ± 2) 10^{-3}	2566 ± 248	(2.6 ± 0.9) 10^{-1}	0.973	
			FA3E			
300	1672 ± 327	(1 ± 1) 10^{-4}	1142 ± 282	(7 ± 4) 10^{-3}	0.967	
350	1534 ± 78	(4 ± 1) 10^{-4}	1422 ± 129	(6 ± 1) 10^{-2}	0.969	
400	991 ± 60	(4 ± 1) 10^{-4}	1807 ± 103	(8 ± 1) 10^{-2}	0.983	
450	1088 ± 103	(1.1 ± 0.4) 10^{-3}	1716 ± 151	(1.2 ± 0.3) 10^{-1}	0.971	
500	518 ± 53	(2.4 ± 0.6) 10^{-3}	2342 ± 79	(2.4 ± 0.2) 10^{-1}	0.994	

parameters with the standard deviation of the least-squares regression parameters as well as the determination coefficients (R^2).

Discussion

The experimental results obtained for fly ash indicate that at temperatures lower than 200 °C, no reaction is observed even with a 24 h reaction time: this indicates the lower temperature limit for the thermal inertization.

Reaction Products in Air. Starting from 250 °C (Table 1), the gasification product is mainly CO_2 ($CO/CO_2 < 0.05$). In the 250−325 °C temperature range quite distinct trace organics are detected: the variability of organic species from different fly ashes is well-known *(12)* and as such was not further investigated.

Role of desorption on reaction products. To clarify the role of organic compounds desorption on kinetics, experiments were performed on FA1, FA2b, and FA3 in a nitrogen flow (Table 1, runs 10−16). The results confirm that thermal desorption of organic compounds occurs under most conditions and depends on fly ash origin and temperature, a fact that must be taken into account in industrial processes for fly ash thermal inertization. However, the mass balance shows that the desorbed organic compounds are in any case less than 5% of TOC^0 content and do not account for the overall toluene-extractable compounds (about 20% for FA3).

The formation of 4−6% of CO_2 was observed in runs 12, 14, and 16. Since no O_2 was present, the formation of CO_2 is surprising but not unexpected *(11)*. As a leak was experimentally excluded, there are two possible explanations: (i) CO_2 is a desorption product and (ii) O_2 is present between the fly ash particles in the loosely packed bed or perhaps adsorbed on the fly ash surface and is supplied by diffusion only. The CO_2 concentration does not change with temperature, and this is compatible with both the first hypothesis and the second one if O_2 is the limiting reagent. However, as the CO_2 formation under nitrogen is not of primary interest in this study, we have not examined the matter closely.

Deconvolution Procedure Performance Evaluation. The best fitting of fly ash TOC-time experimental data at different temperatures was obtained with a sum of two exponentials (eq 1). DSC experiments in the 300−500 °C range allowed us to identify two distinct combustion reactions and to determine their apparent activation energies *(21)*. A similar behavior has already been reported by Stieglitz et al. *(22)*: the rate constants and the temperature trend of the preex-

TABLE 6. Activation (Arrhenius Equation) and Thermodynamic (Eyring Equation) Parameters for Ri and Rj Reactions of FA1, FA2a, FA2b, FA3, FA30, and FA3E[a]

Ri	FA1	FA2a	FA2b	FA3	FA30	FA3E
ln (A/min^{-1})	-(1 ± 1)	-(1 ± 1)	4 ± 2	2 ± 1	2 ± 2	2 ± 1
E_a (kJ mol^{-1})	31 ± 8	33 ± 7	73 ± 12	53 ± 7	52 ± 10	52 ± 8
R^2	0.804	0.732	0.927	0.936	0.965	0.932
$\Delta S^{\ddagger}$ (kJ K^{-1} mol^{-1})	−(0.30 ± 0.01)	−(0.31 ± 0.01)	−(0.26 ± 0.02)	−(0.28 ± 0.01)	−(0.28 ± 0.01)	−(0.28 ± 0.01)
$\Delta H^{\ddagger}$ (kJ mol^{-1})	25 ± 8	27 ± 7	67 ± 12	48 ± 7	47 ± 10	47 ± 8
R^2	0.729	0.663	0.915	0.924	0.958	0.918
$\Delta G^{\ddagger}$ (kJ mol^{-1})	245 ± 8	248 ± 7	253 ± 12	247 ± 7	247 ± 10	248 ± 8

Rj	FA1	FA2a	FA2b	FA3	FA30	FA3E
ln (A/min^{-1})	−(2.1 ± 0.2)	4.6 ± 0.9	−(1.1 ± 0.7)	6.8 ± 0.8	8 ± 1	8 ± 2
E_a (kJ mol^{-1})	10 ± 1	41 ± 5	17 ± 4	52 ± 4	60 ± 6	59 ± 12
R^2	0.943	0.900	0.852	0.976	0.991	0.884
$\Delta S^{\ddagger}$ (kJ K^{-1} mol^{-1})	−(0.311 ± 0.002)	−(0.26 ± 0.01)	−(0.30 ± 0.01)	−(0.237 ± 0.007)	−(0.226 ± 0.009)	−(0.23 ± 0.02)
$\Delta H^{\ddagger}$ (kJ mol^{-1})	5 ± 1	35 ± 5	11 ± 4	47 ± 4	55 ± 6	54 ± 12
R^2	0.754	0.880	0.717	0.969	0.989	0.861
$\Delta G^{\ddagger}$ (kJ mol^{-1})	229 ± 1	220 ± 5	231 ± 4	218 ± 4	218 ± 6	218 ± 12

[a] $\Delta G^{\ddagger}$ at an average temperature of 723 K.

TABLE 7. Deconvolution Parameters C_i, k_i, C_j, and k_j and First-Order Rate Constants k^{mix2} and k^{mix3} for the Reactions of DF−BPh−SiO_2 and DF−BPh−C−SiO_2 Mixtures at Different Temperatures[a]

			DF−BPh−SiO_2				
T (°C)	$C_i \pm \sigma$ (ppm)	$k_i \pm \sigma$ (min^{-1})	$C_j \pm \sigma$ (ppm)	$k_j \pm \sigma$ (min^{-1})	R^2	k^{mix2} (min^{-1})	R^2
75[b]	1793	1.226×10^{-3}	1783	1.226×10^{-3}	0.995	1.258×10^{-3}	0.993
100[b]	1826	3.190×10^{-3}	1717	1.785×10^{-3}	0.999	2.380×10^{-3}	0.999
125[b]	1724	2.093×10^{-3}	1865	8.356×10^{-3}	0.990	4.230×10^{-3}	0.983
150[b]	1572	8.361×10^{-3}	1981	8.358×10^{-3}	1.000	8.373×10^{-3}	1.000
200[b]	1710	1.361×10^{-2}	1790	2.205×10^{-2}	1.000	1.605×10^{-2}	0.997
			DF−BPh-C−SiO_2				
T (°C)	$C_i \pm \sigma$ (ppm)	$k_i \pm \sigma$ (min^{-1})	$C_j \pm \sigma$ (ppm)	$k_j \pm \sigma$ (min^{-1})	R^2	k^{mix3} (min^{-1})	R^2
75[c]	721	6.809×10^{-6}	1146	8.043×10^{-4}	0.998	4.579×10^{-4}	0.996
100[c]	1079	1.91×10^{-6}	825	4.200×10^{-3}	0.977	1.012×10^{-3}	0.939
150[c]	953	7.450×10^{-5}	976	9.986×10^{-3}	0.972	1.413×10^{-3}	0.734
200[c]	942	5.120×10^{-5}	982	2.076×10^{-2}	0.921	1.164×10^{-3}	0.482
350	974 ± 53	$(6 \pm 2) \times 10^{-4}$	891 ± 63	$(3.6 \pm 0.6) \times 10^{-3}$	0.994	1.472×10^{-3}	0.653
400	825 ± 95	$(2.2 \pm 0.5) \times 10^{-3}$	1043 ± 108	$(6 \pm 2) \times 10^{-2}$	0.993	2.943×10^{-3}	0.777
500[c]	1015	5.308×10^{-3}	855	4.074×10^{-1}	0.998	5.487×10^{-3}	0.917
600[c]	736	1.151×10^{-2}	1134	2.574×10^{-1}	0.999	1.411×10^{-2}	0.872

[a] Missing standard errors were not computed due to an ill conditioned matrix. [b] Starting values for the deconvolution procedure were of the same order of magnitude of kinetic constants k_{DF} and k_{BPh} *(13)* and TOC^0_{DF} and TOC^0_{BPh} values in the mixture. [c] Starting values for the deconvolution procedure were of the same order of magnitude of kinetic constants k_C, k_{DF}, and k_{BPh} *(13)* and TOC^0_C and (TOC^0_{DF} + TOC^0_{BPh}) values in the mixture.

ponential parameters as well as DSC results are in a very good general agreement with ours.

In some runs, the trend of experimental points (Figure 1) seems to indicate a first-order behavior; however, the R^2 values reported in Tables 2−5 show that this is not true.

Since a multiparameter (four, in our case) model is not always physically meaningful, it must be carefully evaluated. To do this, we studied the DF−BPh−SiO_2 and DF−BPh−C−SiO_2 model systems. These systems were selected because (i) DF and BPh are PCDF and PCB parent compounds. As pure compounds mixed with SiO_2, DF and BPh have very similar rate constants, k_{DF} and k_{BPh} (Table 6 in ref *13*), and permit an evaluation of the lower limit of the deconvolution procedure; (ii) activated carbon simulates the native carbon in raw fly ash, and (iii) DF−BPh-C−SiO_2 mixture is a model for the fly ash multicomponent system.

DF−BPh−SiO_2 thermal treatment was performed at different temperatures. The experimental data were well fitted with both a first-order equation and a sum of two exponentials. The C_i and C_j parameter values do not depend on temperature (Table 7): their mean values (1725 ± 98 and 1827 ± 101 ppm, respectively) are almost coincident with TOC^0_{DF} and TOC^0_{BPh}, both equal to 1775 ppm. Moreover, at each temperature the rate constant values obtained from the deconvolution are in very good agreement with k_{DF} and k_{BPh} (Table 6 in ref *13*). While the activation and thermodynamic parameters for the first-order scheme (Table 8) are intermediate to those calculated for the pure compounds (Table 7 in ref *13*), those from the deconvolution procedure made it possible to identify k_i with the DF desorption rate constant and k_j with the BPh one.

Thus, the global process is the sum of the thermal desorption of DF and BPh, the temperature independent C_i and C_j parameters have the physical meaning of TOC^0_{DF} and TOC^0_{BPh}, and eq 1 becomes the sum of two independent simultaneous first-order reactions:

$$TOC = TOC^0_{DF} \exp(-k_{DF}t) + TOC^0_{BPh} \exp(-k_{BPh}t) \quad (1a)$$

The experimental data for the DF−BPh−C−SiO_2 mixtures are well fitted by the deconvolution procedure (eq 1), while the R^2 obtained with the first-order equation is always lower than the one obtained with deconvolution (Table 7). Once

TABLE 8. Activation (Arrhenius Equation) and Thermodynamic (Eyring Equation) Parameters for Thermal Treatment of DF−BPh−SiO_2 and DF−BPh−C−SiO_2 Mixtures[a]

DF−BPh−SiO_2	k_i	k_j	k^{mix2}
ln (A/min^{-1})	2 ± 2	5 ± 2	3.1 ± 0.4
E_a (kJ mol^{-1})	26 ± 6	33 ± 5	28 ± 1
R^2	0.851	0.929	0.992
$\Delta S^{\ddagger}$ (kJ K^{-1} mol^{-1})	−(0.27 ± 0.02)	−(0.25 ± 0.01)	−(0.264 ± 0.004)
$\Delta H^{\ddagger}$ (kJ mol^{-1})	23 ± 6	30 ± 5	25 ± 1
R^2	0.813	0.921	0.990
$\Delta G^{\ddagger}$ (kJ mol^{-1})	218 ± 6	211 ± 5	216 ± 3

DF−BPh-C−SiO_2	k_i	k_j
ln (A/min^{-1})	1 ± 1	2 ± 1
E_a (kJ mol^{-1})	39 ± 4	25 ± 3
R^2	0.941	0.929
$\Delta S^{\ddagger}$ (kJ K^{-1} mol^{-1})	−(0.29 ± 0.01)	−(0.27 ± 0.01)
$\Delta H^{\ddagger}$ (kJ mol^{-1})	35 ± 4	21 ± 3
R^2	0.929	0.899
$\Delta G^{\ddagger}$ (kJ mol^{-1})	242 ± 4	219 ± 3

[a] $\Delta G^{\ddagger}$ at an average temperature of 723 K.

again, the C_i and C_j values are independent from temperature (Table 7); the mean values of C_i (906 ± 131 ppm) and C_j (982 ± 121 ppm) are coincident with TOC_C^0 (920 ppm) and the sum (TOC_{DF}^0 + TOC_{BPh}^0) (950 ppm). The rate constants at every temperature are in good agreement with those for the C−SiO_2 mixture, k_C (Table 6 in ref *13*), and the average of k_{DF} and k_{BPh}: the comparison shows that, in the DF−BPh−C−SiO_2 model system, Ri is the carbon oxidation reaction and Rj, the sum of DF and BPh desorption. The activation enthalpy, $\Delta H^{\ddagger}$, and entropy, $\Delta S^{\ddagger}$, values calculated for the DF−BPh−C−SiO_2 mixture (Table 8) are similar to those obtained for C−, DF−, and BPh−SiO_2 mixtures in the higher temperature range (Table 7 in ref *13*).

Thus, the global process is the sum of three independent simultaneous first-order reactions, C oxidation and DF and BPh desorption, but, owing to the very similar k_{DF} and k_{BPh} values, it appears as the sum of only two reactions.

Even the molar free activation energy, $\Delta G^{\ddagger}$, values for the DF−BPh−SiO_2 and DF−BPh−C−SiO_2 mixtures (Table 8) are almost coincident with those calculated for the reactions of the pure compounds not only in value but also in the contribution of the entropic term (more than 80%): therefore, the reaction mechanism is the same both for the pure compounds and their mixtures. These reactions are under a diffusion control with tight transition states (*13*).

Sensitivity analysis and standard errors determined by the procedure identify the limits of deconvolution in distinguishing similar rate constants (as for the DF−BPh−SiO_2 mixture, see Table 7) and determining very little or very high rate constants (e.g. rate constant values for DF−BPh−C−SiO_2 mixture at low and high temperatures, Table 7).

On the basis of these overall results we used deconvolution to process the fly ash kinetic data; the procedure was successfully applied to the TOC vs time data at each temperature (Tables 2−5). The calculated C_i and C_j parameters vary with temperature: this trend is opposite to what observed for model systems (Table 7).

Role of Homogenization and of Organic Compounds on Fly Ash Kinetics. FA3 was ball mill homogenized, while FA30 was not. The homogenization effect on reaction constants does not seem to be particularly important, as the average rate constant ratios k_i(FA30)/k_i(FA3) and k_j(FA30)/k_j(FA3) were 1.3 ± 0.2 and 1.0 ± 0.1. Moreover, the $\Delta H^{\ddagger}$ and $\Delta S^{\ddagger}$ values (Table 6) are "not different". Thus, homogenization does not seem to be a prerequisite for the fly ash thermal treatment for final disposal.

To understand the role of organic compounds on fly ash kinetics, FA3 (TOC^0 = 3525 ppm) was exhaustively extracted with toluene, yielding FA3E (TOC^0 = 2870 ppm). Thus, the contribution of extractable organic carbon to the TOC^0 of FA3 is about 20%. From the kinetic runs performed on FA3E and FA3, both the k_i(FA3E)/k_i(FA3) and k_j(FA3E)/k_j(FA3) ratios are independent from temperature. Their average values (1.1 ± 0.2 for Ri; 0.9 ± 0.3 for Rj) indicate that the organic compounds on fly ash are not the carbon source in Ri or Rj. Even the $\Delta H^{\ddagger}$ or $\Delta S^{\ddagger}$ values are "not different".

Based on the whole of experimental results and the limits of deconvolution procedure, the fate of extractable organic compounds (about 20% of TOC^0 in FA3) can be hypothesized: depending on the reaction temperature, about 10% desorb and/or react. In any case, these processes are negligible in our kinetic study, but they might be of relevant interest in the formation of trace compounds such as PCDD and PCDF. With respect to PCDD/F formation from organic precursors, our results suggest that this mechanism could be not important if the precursors desorb at temperatures lower than the optimal 300−350 °C range for formation.

In conclusion, the experimental kinetic work on fly ash thermal degradation leads to the following observations. The chemical process is the oxidation of carbon to CO_2. We have demonstrated that, under our experimental conditions, the carbon for the reactions is not from organic compounds. The carbon source is likely to originate from the native carbon of MSWI fly ash. The experimental TOC-time data cannot be processed with a standard first-order reaction scheme. Instead, deconvolution with a sum of two exponentials was successfully performed at each temperature. DSC experiments allowed us to identify two distinct combustion reactions (*21*). The large negative $\Delta S^{\ddagger}$ values indicate that the Ri and Rj transition states are more compact and stiffer than the reagent ones. The structural changes are more important than chemical transformations since the entropic term is predominant (for more than 75%) in determining the $\Delta G^{\ddagger}$ values. The key experimental information for the formulation of a reaction scheme is the temperature trend of C_i and C_j parameters (Tables 2−5) where C_i, related to the slower process Ri, decreases while C_j, related to Rj, increases with increasing temperature. This trend is formally similar to that already observed for the thermal degradation of OCDF spiked on fly ash (*23*), but it is not observed for DF−BPh−SiO_2 and DF−BPh−C−SiO_2 mixtures (Table 7). All this requires a generalized kinetic model that reflects this variety of experimental results.

In part 2 of this work (*17*), the empirical reaction rates determined in the experiments here reported are used to develop a kinetic scheme to predict the thermal degradation rate of fly ash native carbon.

Acknowledgments

We thank Massimo Ferri for his valuable work in the laboratory, the "Fondazione Lombardia per l'Ambiente", and the Italian National Research Council for financial support (Grant 95.00552.CT13).

Supporting Information Available

A listing of TOC vs time data at different temperatures for FA1, FA2a, Fa2b, FA3, FA30, and FA3E samples (Tables S1−S6), DF−BPh−SiO_2 (Table S7), and DF−BPh−C−SiO_2 (Table S8) mixtures. This material is available free of charge via the Internet at http//pubs.acs.org.

Literature Cited

(1) Pitea, D.; Bonati, L.; Cosentino, U.; Lasagni, M.; Moro, G. *Toxicol. Environ. Chem*. **1989**, *23*, 239−261.
(2) Fiedler, H. *Organohalogen Compd*. **1993**, *11*, 221−228.
(3) Vogg, H.; Stieglitz, L. *Chemosphere* **1986**, *15*, 1373−1378.
(4) Addink, R.; Olie, K. *Environ. Sci. Technol.* **1995**, *29*, 1586−1590.
(5) Ismail, J. M. K.; Walker, Jr., P. L. *Carbon* **1989**, *27*, 549−559.
(6) Stieglitz, L.; Vogg, H.; Zwick, G.; Beck, J.; Bautz, H. *Chemosphere* **1991**, *23*, 1255−1264.
(7) Schwarz, G.; Stieglitz, L. *Chemosphere* **1992**, *25*, 277−282.
(8) Milligan, M. S.; Altwicker, E. *Environ. Sci. Technol.* **1993**, *27*, 1595−1601.
(9) Milligan, M. S.; Altwicker, E. *Carbon* **1993**, *31*, 977−986
(10) Huang H.; Buekens A. *Sci. Total. Environ*. **1997**, *193*, 121−141.
(11) Addink, R.; Olie, K. *Environ. Sci. Technol.* **1995**, *29*, 1425−1435.
(12) Cains, P. W.; McCausland, L. J.; Fernandes, A. R.; Dyke, P. *Environ. Sci. Technol.* **1997**, *31*, 776−785.
(13) Lasagni, M.; Collina, E.; Tettamanti, M.; Pitea, D. *Environ. Sci. Technol.* **1996**, *30*, 1896−1901.
(14) Lasagni, M.; Cosentino, U.; Moro, G.; Pitea, D. In *Trends in Ecological Physical Chemistry*; Bonati, L., Cosentino, U., Lasagni, M., Moro, G., Pitea, D., Schiraldi, A., Eds.; Elsevier: Amsterdam, 1993; pp 253−274.
(15) Lasagni, M.; Collina, E.; Tettamanti, M.; Ferri, M.; Pitea, D. *Organohalogen Compd*. **1993**, *11*, 199−202.
(16) Lasagni, M.; Collina, E.; Ferri, M.; Tettamanti, M.; Pitea, D. *Waste Manage. Res.* **1997**, *15*, 507−521
(17) Collina, E.; Lasagni, M.; Tettamanti, M.; Pitea, D. *Environ. Sci. Technol.* **2000**, *34*, 137−142.
(18) Fermo, P.; Cariati, F.; Pozzi, A.; Demertin, F.; Tettamanti, M.; Collina, E.; Lasagni, M.; Pitea, D.; Puglisi, O.; Russo, U. *Fresenius' J. Anal. Sci*., in press.
(19) Nelder, J. A.; Mead, R. *Comput. J.* **1965**, *7*, 308−313.
(20) Zar, J. H. *Biostatistical Analysis*, 2nd ed.; Prentice-Hall: NJ, 1984.
(21) Tettamanti, M.; Collina, E.; Lasagni, M.; Pitea, D.; Grasso, D.; La Rosa, C. *Termochim. Acta* **1998**, *321*, 133−141.
(22) Stieglitz, L.; Eichberger, M.; Schleihauf, J.; Beck, J.; Zwick, G.; Will, R. *Chemosphere* **1993**, *27*, 343−350.
(23) Collina, E.; Lasagni, M.; Pitea, D.; Keil, B.; Stieglitz, L. *Environ. Sci. Technol.* **1995**, *29*, 577−585.

Received for review December 4, 1998. Revised manuscript received October 14, 1999. Accepted October 19, 1999.

ES981264C